SIAM J. APPL. MATH.
Vol. 70, No. 6, pp. 2075–2096

THE SHAPE OF A SMALL LIQUID DROP ON A CONE AND PLATE RHEOMETER*

V. CREGAN†, S. B. G. O'BRIEN†, AND S. MCKEE‡

Abstract. We construct asymptotic solutions for the shape of a small liquid sessile drop in a cone and plate rheometer. The approximation is based on small Bond number or, equivalently, on a characteristic length scale which is much smaller than the capillary length. The drop has a complicated asymptotic structure, consisting of five separate scalings, which is resolved using the method of matched asymptotic expansions. We find that the presence of a substrate above (and below) the drop gives rise to qualitatively new drop configurations.

Key words. liquid bridge, sessile drop, pendant drop, asymptotics, surface tension, curvature, matched asymptotic expansions

AMS subject classifications. 34E10, 76B45, 76A02

DOI. 10.1137/090765201

1. Introduction.

The topic of capillarity and surface tension has long been of interest to applied mathematicians and other scientists, as evidenced by the pioneering work of Pierre Simon de Laplace and Thomas Young. More recently de Gennes, Brochard-Wyart, and Quéré produced a significant research monograph [6]. In practice, surface tension phenomena play an important role in climate, plant physiology, and porous flow, and the chemical, glass (e.g., [10]), and automobile industries. Capillarity studies the interfaces between immiscible fluids. Such interfaces are free to change shape in order to minimize their surface energy and can be thought of as being membranes in tension with the surface tension acting to oppose the distortion. It was Gauss, who, while verifying the semiheuristic approach of Laplace, characterized capillarity problems in terms of energies, in particular, using the principle of virtual work. Using this approach, many capillarity problems can be formulated as extremal problems in the calculus of variations: the associated Euler–Lagrange equation can then be identified with the differential equation originally derived by Laplace and Young. The latter is the approach taken in the present paper.

The Laplace–Young capillary equation which models a balance between gravity and surface tension effects is nonlinear, and no closed form solution is available. Hence, the usual approach to capillary problems has been either numerical or asymptotic [1], [3], [4], [21] (see also Figure 1 for what is effectively a numerical computation). In the present paper, we construct an asymptotic solution for the shape of a static liquid drop on a cone and plate rheometer (see Figure 2) with a view to using this as the initial condition for advanced numerical simulations involving non-Newtonian fluids.

A cone and plate rheometer (see Figure 2) is a laboratory device used to measure the way in which a liquid, suspension, or slurry flows in response to applied forces. The

*Received by the editors July 15, 2009; accepted for publication (in revised form) January 5, 2010; published electronically April 2, 2010. This work was supported by the Mathematics Applications Consortium for Science and Industry (www.macsi.ul.ie) funded by the Science Foundation Ireland mathematics initiative grant 06/MI/005 and an Embark Initiative grant (RS/2006/41).
http://www.siam.org/journals/siap/70-6/76520.html

†MACSI, Department of Mathematics, University of Limerick, Limerick, Ireland (vincent.cregan@ul.ie, stephen.obrien@ul.ie).

‡Department of Mathematics, University of Strathclyde, Glasgow, G1 1XH, Scotland (s.mckee@strath.ac.uk).

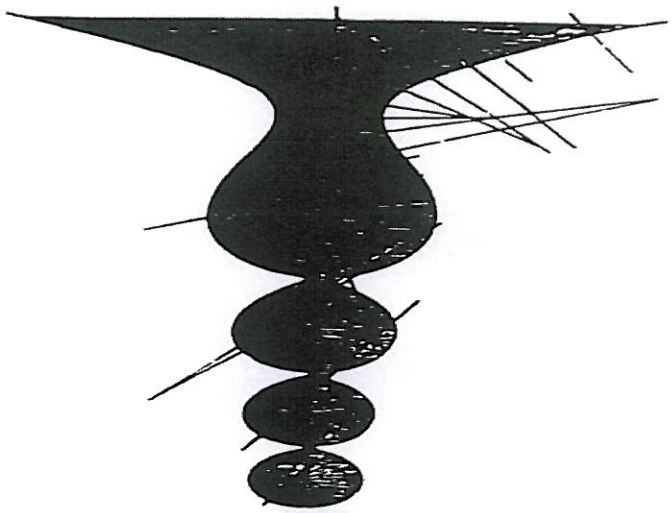

FIG. 1. *Lord Kelvin's multiple pendant drop.*

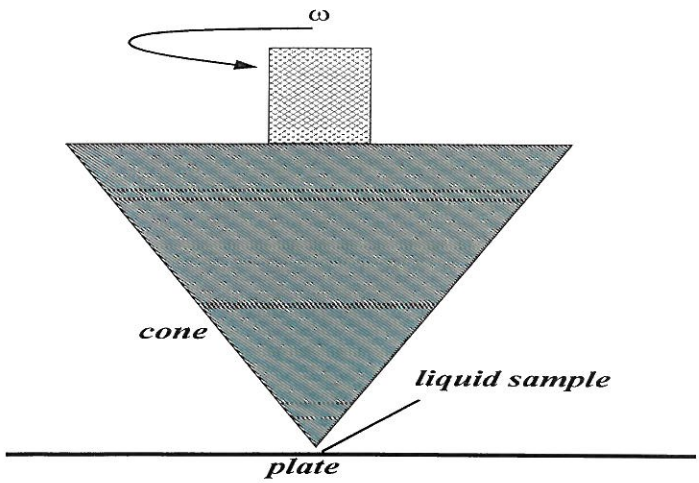

FIG. 2. *Schematic of a cone and plate rheometer.*

liquid is placed on a circular horizontal plate, and a shallow cone is lowered into the liquid. The angle between the surface of the cone and the plate is typically small. The cone is usually designed with an angle of less than 10^0. The test fluid is constrained in

the narrow gap between the two surfaces. Typically, the plate is rotated and the force on the cone measured (though either may rotate depending on instrument design). On the basis of the measured forces, various properties of the liquid can be inferred (e.g., for the case of a Newtonian liquid, its viscosity). In practice, cone and plate and parallel plate measurement tools are most often used for highly viscous pastes, gels, and concentrated suspensions. In Figure 3, we sketch a cartoon of a drop at the beginning of an experiment. The diagram is not to scale. In addition, the details of the drop shape will be determined by the contact angles which the drop makes with both the cone and plate. In practice, these angles are often the same.

We previously showed how matched asymptotic expansions could be used to obtain closed form expressions for "small" static liquid drops (more precisely for the case of small Bond number) [17], [11]. In the present case, we use a sessile drop formulation, i.e., we consider the drop as resting on a plate. The novel feature is that the traditional sessile drop is smooth and flat at its apex: in the present instance the top of the drop is distorted by the cone of the rheometer. We will see that this opens out the drop and, in theory, can give rise to multiple drop solutions at the base of the original drop similar to those obtained for the pendant problem [14], [12]. It is interesting that the traditional sessile drop does not allow such solutions (see [17], [11]); i.e., the distortion caused by the cone has significant consequences for the global behavior of the drop.

2. Governing equations. The Laplace–Young equation describing the equilibrium of a free liquid gas interface is a statement that the mean curvature of the free surface is proportional to the pressure change across the interface. The liquid gas interface involved has a surface tension γ and density difference ρ and hence an associated capillary length $a \equiv \sqrt{\frac{\gamma}{\rho g}}$, where g is the acceleration due to gravity. Note that an air-water interface has a capillary length of about 2.7mm.

Consider a sessile drop resting on a horizontal substrate [17] as in Figure 4. Assuming that the contact angle is constant, the resulting drop will be axisymmetric with profile $z^* = z^*(r^*)$ with respect to a polar coordinate system. If p^* is the pressure at the point $z^* = 0$ (where the z^* axis points downward from the top of the drop), then the pressure field will be hydrostatic and will be given by $p^* + \rho g z^*$.

While the traditional formulation for a sessile drop defines p^* in terms of the unknown equal radii of curvature at the top of the drop (Figure 4), this is unnecessary and inappropriate for the case under consideration in the present paper, sketched in Figure 3. Instead, we simply treat p^* as an unknown constant to be determined in the course of the analysis. It is the pressure at some arbitrary reference height in the drop. In the present case, we choose this to be the point in the neck at the top of the drop (Figure 3) where the drop is inclined vertically (i.e., at the thinnest point of the neck).

A significant body of work on capillary problems has been produced by Concus and Finn [3], summarized in [4], and generalized by other authors [1]. Concus and Finn examine in detail the global behavior of solutions and some asymptotic limits. They use a different formulation of the problem by shifting the X axis. From a mathematical point of view, this is a formal simplification, but, in fact, there are difficulties hidden in this approach since this height is essentially a pressure which in the present formulation would have to be determined as part of the solution [19]. Indeed, in the introduction of [3] it is pointed out that the determination of this pressure term (referred to as a Lagrange multiplier) may lead to technical difficulties. Such difficulties do not arise in the approach of the present paper, where the pressure

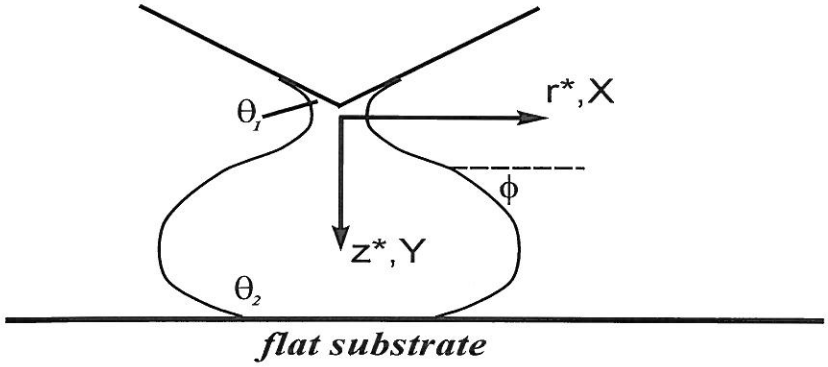

FIG. 3. *Schematic of the drop profile.*

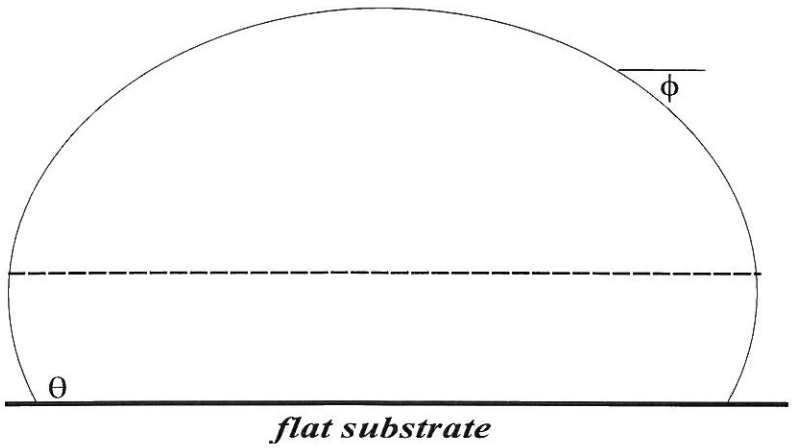

FIG. 4. *A "traditional" sessile drop.*

term is explicitly calculated in the appropriate asymptotic limit. In [3] the apparent drop height $u_0(\sim 2/\varepsilon$ of the present paper) is given as a boundary condition, and some asymptotic results are obtained in the limit of large drop height. In effect this is a type of inverse formulation, i.e., the assumed pressure jump then fixes the overall shape of the drop. In the limit of large pressure jumps, the lowest drops are then "small," and this provides the link with the asymptotics of the present paper.

At any point along the interface, the pressure is balanced by the capillary effects

giving rise to

$$\gamma\left(\frac{1}{R_1}+\frac{1}{R_2}\right)=p^*+\rho g z^*, \tag{1}$$

where R_1, R_2 are the principle radii of curvature. The first of these is associated with the drop curvature when viewed in profile; the second is the curvature in a perpendicular plane containing the normal. In cylindrical polars, (1) becomes

$$\gamma\left(\frac{z^{*\prime\prime}}{(1+z^{*\prime 2})^{\frac{3}{2}}}+\frac{z^{*\prime}}{r^*(1+z^{*\prime 2})^{\frac{1}{2}}}\right)=p^*+\rho g z^*. \tag{2}$$

In the literature (e.g., [7]), it has become the custom to present the equation in terms of dimensionless variables X, Y, P:

$$z^*=Ya, \quad r^*=Xa, \quad p^*=P\rho g a, \tag{3}$$

where $a \equiv \sqrt{\gamma/(\rho g)}$ is the capillary length. As a number of rescalings will occur later, it is useful to have fundamental dimensionless variables to which we can refer during the later asymptotic matching. The dimensionless version of (2) is then

$$\frac{Y''}{(1+Y'^2)^{\frac{3}{2}}}+\frac{Y'}{X(1+Y'^2)^{\frac{1}{2}}}=P+Y. \tag{4}$$

This dimensionless equation does not capture any significant asymptotic balances: it should be regarded as a neutral nondimensionalization to keep us in line with previous authors (e.g., [7]).

We note that L (see [11], [19]) is the dimensional drop half-width—an observable quantity—and the corresponding dimensionless quantity is $L/a \equiv \varepsilon$. This direct formulation with $Y = Y(X)$ has the advantage that the particular physical balances are easy to understand.

From a numerical point of view, a more convenient parametric formulation uses the arclength as parameter (and independent variable); the dependent variables are $X(s), Y(s)$, and the inclination $\phi = \phi(s)$. In this case the dimensionless system is

$$\frac{d\phi}{ds}+\frac{\sin\phi}{X}=P+Y, \quad \frac{dX}{ds}=\cos\phi, \quad \frac{dY}{ds}=\sin\phi, \tag{5}$$

where the dimensional arclength is $s^* = sa$, and the inclination $\phi(s)$ is left unscaled.

2.1. Dimensionless formulation for asymptotic analysis. The Laplace–Young equation can also be written in the following convenient form by eliminating the dimensionless arclength s from (5):

$$\begin{aligned}\frac{dX}{d\phi}&=\frac{X\cos\phi}{XP+XY-\sin\phi},\\ \frac{dY}{d\phi}&=\frac{X\sin\phi}{XP+XY-\sin\phi},\end{aligned} \tag{6}$$

where X, Y are the dimensionless radial and axial coordinates, P is the dimensionless pressure measured from some arbitrary point, and ϕ is the angle of inclination of the profile. This particular formulation will be the starting point of our analysis.

If we were dealing with the simple sessile drop in Figure 4, $\phi = 0, X = 0, Y = 0$ at the top of the drop with the Y axis pointing vertically downward. ϕ then increases to $\pi/2$ at the point where the drop profile becomes vertical, etc. In this formulation, X, Y are thus regarded as functions of the independent variable ϕ. However, it is necessary to derive any turning points of the dependent variable ϕ. Although the angle ϕ increases monotonically for the simple sessile drop of Figure 4, this is not the case for the more complicated situation of Figure 3, which we are about to examine. Note that the arclength formulation of (5) avoids this complication: arclength increases monotonically.

In the problem to be studied in the present paper (see Figure 3), we require three boundary conditions: in effect, one for each ODE of (6), and a third to fix the constant P, the pressure at the point in the neck at the top of the drop where the profile becomes vertical and X attains a local minimum. From previous work [11], [12], it is convenient to assume that the thickness of the neck is $O(\varepsilon^3)$. This will be verified by the matching, in any case, so we choose to start the solutions from the point of minimum width in the neck. The contact angles play a role in that they provide truncation points. By way of illustration, let us consider the simple sessile drop of Figure 4. If the contact angle between liquid and plate is $\pi/2$, then we truncate the drop along the dashed line, and the continuation below that line is purely mathematical in nature.

Hence, we will start up our solutions for the case in Figure 3, using the following conditions:

$$X(\phi = \pi/2) = \alpha\varepsilon^3, \quad Y(\phi = \pi/2) = 0; \tag{7}$$

though we will also require that $X(\phi = \pi/2) = \varepsilon$ in the main drop (Figure 5), where $\varepsilon = L/a = \sqrt{\frac{L^2\rho g}{\gamma}}$ is the dimensionless half-width and may also be considered a Bond number. For the moment, we will treat α as a free $O(1)$ parameter, but we will have more to say about this in due course. It is important to realize that the solutions can be extended upward, as would clearly be required for the situation in Figure 3, where the upper contact angle $\theta_1 \approx 0$. We will seek asymptotic solutions for the case $\varepsilon \ll 1$, which physically corresponds to the drop half-width being much smaller than the capillary length.

Recent authors have tended to use the drop width as a characteristic length scale because it is an experimentally easily determinable quantity [11], [19], [18], [13]. In [3], solutions are analyzed both asymptotically and numerically, but while bounds are placed on the location of vertical points the actual drop shapes are not derived. The advantage of the approach in the present paper is that we consider the appropriate balances in the different regions using matched asymptotic expansions, and this approach allows an explicit (albeit parametric) description of the drop profile.

3. Asymptotic structure of the solutions. The basic asymptotic behavior for problems of this type has been discussed at length in [12], [11]. Note that the drop has a neck, an upper boundary layer, and an outer region with another (lower) boundary layer at the base (see Figure 5 for the basic scales).

3.1. The neck. In the upper neck of Figure 5, there is a balance between the curvature (surface tension) terms which are of opposite sign (locally the surface is a saddle), and it is described by the following rescaling:

$$X = \varepsilon^3 u, \quad Y = \varepsilon^3 v, \quad P = p/\varepsilon, \quad \phi = O(1), \tag{8}$$

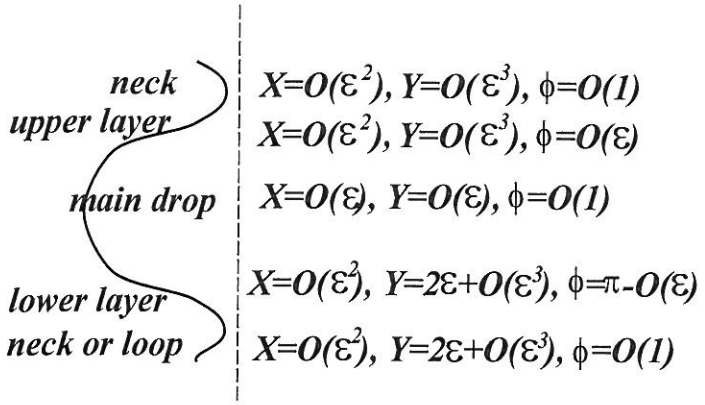

FIG. 5. *Asymptotic regions in the drop. (Not to scale.)*

where u, v, p are the rescaled variables. In terms of the boundary conditions (7), we then have $u(\phi = \pi/2) = \alpha$, $v(\phi = \pi/2) = 0$. At leading order, the pressure term P plays no role and the leading order equations are

$$\frac{du}{d\phi} = -u \cot \phi, \tag{9}$$

$$\frac{dv}{d\phi} = -u. \tag{10}$$

The corresponding solutions are

$$u = \alpha \csc \phi, \tag{11}$$

$$v = -\alpha \ln |\tan \phi/2| . \tag{12}$$

As $\phi \downarrow 0$, a singularity occurs, and a boundary layer (upper) containing a point of inflection also occurs.

3.2. Upper boundary layer. The upper boundary layer (Figure 5) provides a transition between the curvature dominated terms of the neck and the three term balance of the main drop. We rescale as follows:

$$X = \varepsilon^2 \xi, \quad Y = \varepsilon^3 \zeta, \quad P = p/\varepsilon, \quad \phi = \varepsilon \Phi, \tag{13}$$

where ξ, ζ, Φ are the new variables. It is simplest at this point to predict that $p \sim 2$, as in previous work. This will be corroborated later by the matching. The leading order balance is now given by

$$\frac{d\xi}{d\Phi} = \frac{\xi}{\xi p - \Phi}, \tag{14}$$

with solution

$$\Phi = \xi - \frac{C}{\xi} \text{ or } \xi = \frac{1}{2}\left(\Phi \pm \sqrt{(\Phi^2 + 4C)}\right). \tag{15}$$

It transpires that $C < 0$, and there is a point of inflection at the point $\Phi = \sqrt{-4C}$. The negative root of (15) is appropriate before this point, where ϕ is decreasing to $\varepsilon\sqrt{-4C}$. After inflection, the positive root is the relevant one, and ϕ increases once more.

The scaled Y equation to leading order is

$$\frac{d\zeta}{d\Phi} = \frac{\Phi\xi}{\xi p - \Phi}, \tag{16}$$

with solution

$$\zeta = \frac{1}{4}\Phi^2 - \frac{1}{4}\Phi\sqrt{(\Phi^2 + 4C)} - \alpha \ln\left(\Phi + \sqrt{(\Phi^2 + 4C)}\right) + c_1 \tag{17}$$

before the point of inflection. After inflection, the solution is

$$\zeta = \frac{1}{4}\Phi^2 + \frac{1}{4}\Phi\sqrt{(\Phi^2 + 4C)} + \alpha \ln\left(\Phi + \sqrt{(\Phi^2 + 4C)}\right) + c_2. \tag{18}$$

It is convenient to rewrite this in the equivalent form as

$$\zeta = \frac{1}{4}\Phi^2 + \frac{1}{4}\Phi\sqrt{(\Phi^2 + 4C)} - \alpha \ln\left(\Phi - \sqrt{(\Phi^2 + 4C)}\right) + c_3 \tag{19}$$

using the identity

$$-\ln\left(\Phi - \sqrt{\Phi^2 + 4C}\right) \equiv \ln\left(\Phi + \sqrt{\Phi^2 + 4C}\right) - \ln(-4C), \tag{20}$$

as continuity at the inflection point now merely requires that $c_1 = c_3$.

3.3. Matching of neck and upper boundary layer. Asymptotic matching was carried out using the extended van Dyke system [22], which is especially appropriate for this problem, where terms arise which are logarithmic in the small parameter ε, and the simple counting of terms is dangerous. For the purposes of matching, it is useful to write the solutions in terms of the fundamental dimensionless variables X, Y, ϕ. Thus for the X equations of the neck and upper boundary layer (see Figure 5), we must match

$$X = \alpha\varepsilon^3 \csc\phi \quad \text{and} \quad X = \frac{1}{2}\varepsilon^2\left(\Phi \pm \sqrt{\Phi^2 + 4C}\right) \quad \text{with } \phi = \varepsilon\Phi. \tag{21}$$

Matching gives the following result:

$$C = -\alpha. \tag{22}$$

As $\alpha > 0$, this apparently innocuous result is significant in that a negative value of C means that an inflection point occurs. This should be compared with previous sessile drop solutions [11], where the different initial conditions at the top of the drop ($X = Y = \phi = 0$) precluded such behavior, and the inclination ϕ increased monotonically from zero toward π. At the base of the traditional sessile drop of Figure 4, there is indeed a boundary layer, but no inflection point occurs and the inclination ϕ continues increasing monotonically.

The Y matching compares

$$\begin{aligned} Y &= -\alpha\varepsilon^3 \ln\left|\tan(\phi/2)\right|, \\ Y &= \varepsilon^3\left(\frac{1}{4}\Phi^2 - \frac{1}{4}\Phi\sqrt{(\Phi^2 + 4C)} - \alpha \ln\left(\Phi + \sqrt{(\Phi^2 + 4C)}\right) + c_1\right), \\ \phi &= \varepsilon\Phi, \end{aligned} \tag{23}$$

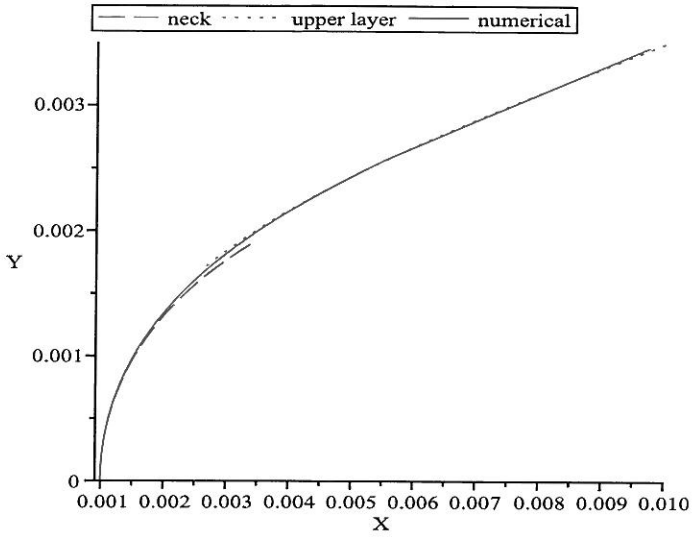

FIG. 6. *Upper neck and boundary layer asymptotic solution compared to the numerical solution (solid line) of* (5). $\varepsilon = 0.1, \alpha = 1$.

and we can represent the final result formally by choosing

$$c_1 = -\frac{1}{2}\alpha(1 - 4\ln 2 + 2\ln\varepsilon). \tag{24}$$

However this apparently simple result masks the occurrence of switchback terms (see [8]). Of course, c_1 in (23) was derived on the basis that it was a pure constant (independent of ε). In the appendix, we give the technical justification and demonstrate that there are extra terms proportional to $\ln\varepsilon$ whose existence is required by the matching. For convenience of presentation, here they have been absorbed into the "constant" c_1.

In Figure 6 we compare the upper neck solutions with numerical computations of (5).

3.4. The main drop and matching with the upper boundary layer. In the main body of the drop (Figure 5), the basic shape is nearly spherical, and the fundamental balance is between the two curvature terms of (4), which are now approximately equal ($\sim 1/\varepsilon$) and of the same sign, and the pressure term $P \sim 2/\varepsilon$. To reflect this, we rescale via

$$X = \varepsilon x, \quad Y = \varepsilon y, \quad P = p/\varepsilon, \tag{25}$$

and the rescaled equations are

$$\frac{dx}{d\phi} = \frac{x\cos\phi}{\varepsilon^2 xy + xp - \sin\phi}, \tag{26}$$

$$\frac{dy}{d\phi} = \frac{x\sin\phi}{\varepsilon^2 xy + xp - \sin\phi}. \tag{27}$$

For meaningful matching with the upper boundary layer, it is necessary to expand to first order, so we seek solutions of the form

$$x \sim x_0 + \varepsilon^2 x_1, \quad y \sim y_0 + \varepsilon^2 y_1, \quad p \sim p_0 + \varepsilon^2 p_1. \tag{28}$$

At leading order we find that

$$x_0 p_0 x_0' - x_0' \sin\phi = x_0 \cos\phi, \tag{29}$$

with general solution

$$x_0 = \frac{\sin\phi \pm \sqrt{\sin^2\phi - 2p_0 c_4}}{p_0}. \tag{30}$$

Matching with the upper boundary layer solution and the requirement that $x_0(\phi = \pi/2) = 1$ shows that $c_4 = 0, p_0 = 2$. Thus, we will use this fact to simplify the presentation of the results. The leading order Y equation is

$$x_0 p_0 y_0' - y_0' \sin\phi = x_0 \sin\phi, \tag{31}$$

with solution

$$y_0 = c_5 - \cos\phi. \tag{32}$$

Leading order matching trivially shows that $c_5 = 1$.

At the next order, the X equation is

$$x_0 y_0 x_0' + x_0 p_1 x_0' + x_1 p_0 x_0' + x_0 p_0 x_1' - x_1' \sin\phi = x_1 \cos\phi, \tag{33}$$

with solution

$$x_1 = \frac{1}{12}\frac{3(1+p_1)\cos(2\phi) - 4\cos^3\phi + 12c_6}{\sin\phi}. \tag{34}$$

For future reference, we note that as $\phi \to \pi$, the behavior of x_1 will become singular by virtue of the sine term in the denominator, unless the numerator satisfies certain conditions. Noting that

$$x_1 \sim \frac{\frac{7}{12} + \frac{p_1}{4} + c_6}{\pi - \phi} - \left(\frac{65}{72} + \frac{11p_1}{24} - \frac{c6}{6}\right)(\pi - \phi) + O(\pi - \phi)^2, \tag{35}$$

the solution will become singular unless

$$\frac{7}{12} + \frac{p_1}{4} + c_6 = 0, \tag{36}$$

in which case

$$\lim_{\phi \to \pi} x_1 = 0. \tag{37}$$

In this case x_1 can be written in the form as

$$x_1 = -\frac{1}{6\sin\phi}\left(5 + 3p_1 + 2\cos^3\phi - 3\cos^2\phi - 3p_1\cos^2\phi\right). \tag{38}$$

For future reference, if $p_1 = -5/3$, then this can be further simplified to

$$x_1 = -\frac{\cos^2\phi\cos\frac{\phi}{2}}{3\sin\frac{\phi}{2}}. \tag{39}$$

Matching the outer and the upper boundary layer solution leads to comparing

$$X = \varepsilon^2\left(\Phi + \frac{3p_1 + 12c_6}{12\Phi}\right), \tag{40}$$

$$X = \varepsilon^2\left(\Phi - \frac{\alpha}{\Phi}\right), \tag{41}$$

$$\phi = \varepsilon\Phi, \tag{42}$$

and matching requires

$$c_6 = \frac{1}{12} - \frac{p_1}{4} - \alpha. \tag{43}$$

α and p_1 are still free parameters at this point. The Y equation is

$$x_0y_0y_0' + x_0p_1y_0' + x_1p_0y_0' + x_0p_0y_1' - y_1'\sin\phi = x_1\sin\phi, \tag{44}$$

with solution

$$y_1 = -\frac{1}{3}\cos^2\phi + \frac{1}{3}\ln|\sin\phi| + \frac{1}{2}\cos\phi + \left(\alpha - \frac{1}{3}\right)\ln\left|\tan\frac{\phi}{2}\right| + \frac{1}{2}p_1\cos\phi + c_7. \tag{45}$$

It is convenient to rewrite y_1 as follows:

$$y_1 = -\frac{1}{3}\cos^2\phi + \frac{1}{3}\ln 2 + \alpha\ln\left|\sin\frac{\phi}{2}\right| + \left(\frac{2}{3} - \alpha\right)\ln\cos\frac{\phi}{2} + \frac{1}{2}\cos\phi + \frac{1}{2}p_1\cos\phi + c_7, \tag{46}$$

in order to observe that this will become singular as $\phi \to \pi$, unless $\alpha = 2/3$. Matching with the upper boundary layer solution compares

$$Y = \varepsilon^3\left(\frac{1}{4}\Phi^2 + \frac{1}{4}\Phi\sqrt{\Phi^2 - 4\alpha} - \alpha\ln\left(\Phi - \sqrt{(\Phi^2 - 4\alpha)}\right) + c_1\right), \tag{47}$$

$$Y = \varepsilon(1 - \cos\phi) + \varepsilon^3\left(-\frac{1}{3}\cos^2\phi + \frac{1}{3}\ln|\sin\phi| + \frac{1}{2}\cos\phi + \left(\alpha - \frac{1}{3}\right)\ln\left|\tan\frac{\phi}{2}\right| + \frac{1}{2}p_1\cos\phi + c_7\right), \tag{48}$$

$$\phi = \varepsilon\Phi, \tag{49}$$

where c_1 is given by (24). Here, it is again important to use extended van Dyke matching. This leads to the need to include switchback terms of $O(\varepsilon^3\ln\varepsilon)$ (see the appendix), and we can represent the final matching result formally as

$$c_7 = -\frac{1}{6} + \left(2\alpha - \frac{1}{3}\right)\ln 2 - \frac{1}{2}p_1 - \alpha - \alpha\ln\alpha - 2\alpha\ln\varepsilon. \tag{50}$$

Again, for future reference, we note that as $\phi \to \pi$, y_1 will become singular via the logarithmic terms, unless

$$\alpha = \frac{2}{3}. \tag{51}$$

In Figures 7, 8, and 9 we compare the asymptotic outer solution with numerically computed solutions using the alternative parametric approaches of (5) and (6). Elsewhere we invariably use the arclength formulation (5) for numerical computations. Figures 8 and 9 are included to show how the asymptotic solutions improve for decreasing ε.

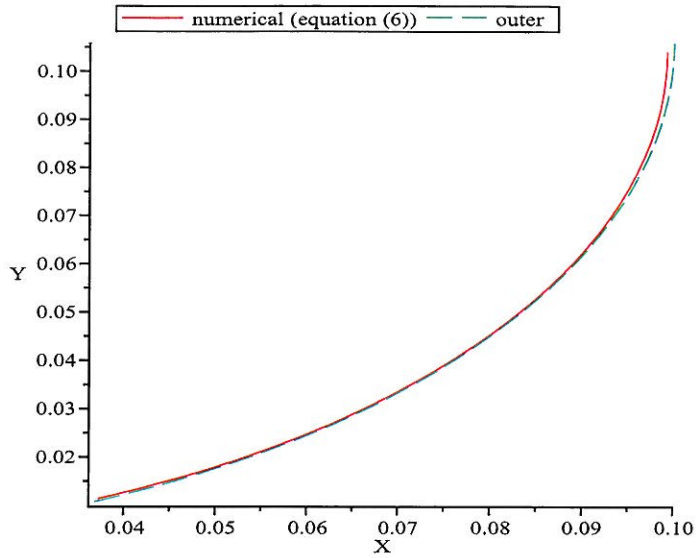

FIG. 7. *Outer solution (dashed line) compared to numerical solution of the parametric formulation of* (6) *using the inclination* ϕ *as parameter.* $\varepsilon = 0.1, \alpha = 1$.

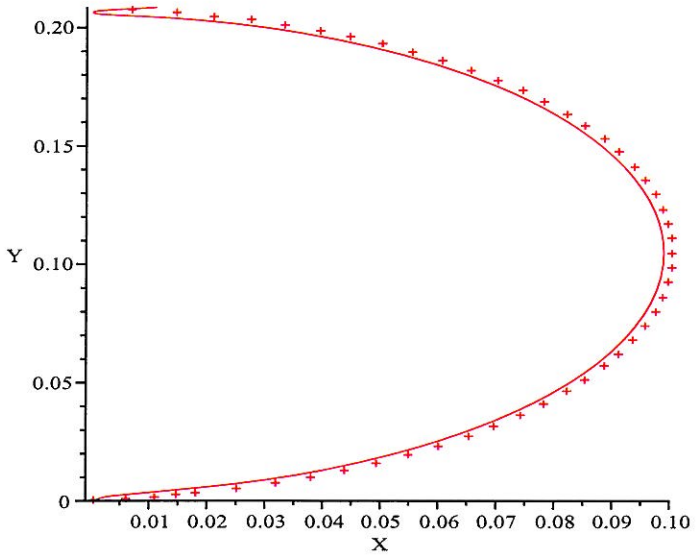

FIG. 8. *Outer solution compared to the numerical solution (solid line) of the problem using the arclength formulation* (5). $\varepsilon = 0.1, \alpha = 1$.

3.5. The lower boundary layer. In the case of the traditional sessile drop of Figure 4, it was shown in [11] that if the contact angle approaches π, a new boundary

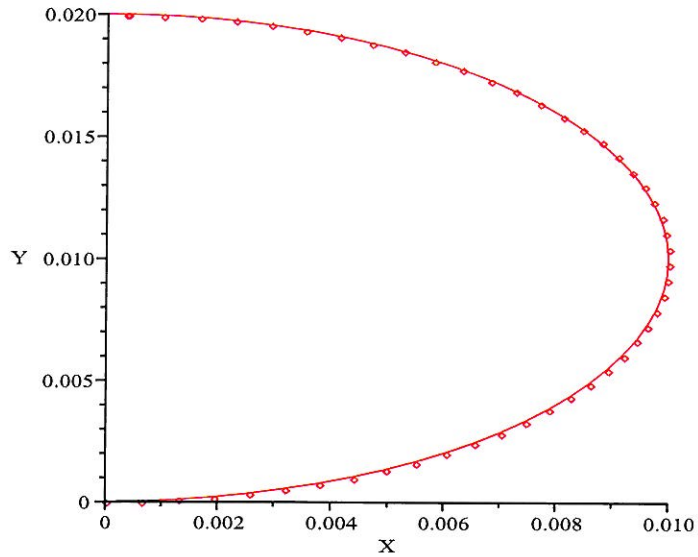

FIG. 9. *Outer solution compared to the numerical solution (solid line) of the arclength formulation* (5). $\varepsilon = 0.01, \alpha = 2/3$.

layer must be inserted at the base of the drop. Here, too, at the bottom of the main drop (see Figure 5), we rescale as follows

$$X = \varepsilon^2 \xi, \quad Y = 2\varepsilon + \varepsilon^3 \zeta, \quad \phi = \pi - \varepsilon\Phi, \quad P = p/\varepsilon. \tag{52}$$

The leading order X equation is

$$\frac{d\xi}{d\Phi} = \frac{\xi}{\xi p - \Phi}, \tag{53}$$

with solution

$$\Phi = \xi - \frac{D}{\xi} \quad \text{or} \quad \xi = \frac{1}{2}\left(\Phi \pm \sqrt{(\Phi^2 + 4D)}\right). \tag{54}$$

The sign of D determines whether there is an inflection point in the layer. From a mathematical point of view, it transpires that all three possibilities $D > 0, D < 0, D = 0$ can arise. The particular value that is selected turns out to depend on the value of α in (7). Up to this point we have two free parameters α, D. We have not yet imposed the boundary condition that $X(\phi = \pi/2) = \varepsilon$, which implies that $x_1(\phi = \pi/2) = 0$. Referring back to (38), this gives us the extra condition

$$p_1 = -\frac{1}{3} - 2\alpha, \tag{55}$$

and we further deduce that

$$D = \frac{2}{3} - \alpha. \tag{56}$$

Thus we see that

$$\alpha > 2/3 \Longrightarrow D < 0, \quad \alpha = 2/3 \Longrightarrow D = 0, \quad \alpha < 2/3 \Longrightarrow D > 0. \tag{57}$$

In particular, we note that $\alpha = 2/3$ corresponds to the special cases (36) and (51) referred to in section 3.4.

3.5.1. $D = 0$. If $\alpha = 2/3$, then $D = 0$, and the leading order equations are (54) and

$$\frac{d\zeta}{d\Phi} = -\Phi. \tag{58}$$

These have the simple solutions

$$\zeta = -\frac{1}{2}\Phi^2 + A, \qquad \xi = \Phi, \tag{59}$$

and we notice that $\frac{d\zeta}{d\xi} = -\Phi$. A little reflection suggests that there is in fact no boundary layer because x_1 and y_1 of the outer solution both remain finite as $\phi \to \pi$. In this case, the outer solutions of the previous section remain valid, and it is easy to show that

$$x_1, X \to 0, \quad \frac{dY}{dX} \to 0, \quad (\phi \to \pi), \tag{60}$$

and the drop terminates smoothly at $X = 0$ for some finite Y value. Here we have in fact recovered a traditional pendant drop solution [11] (where the base of the drop is free, i.e., there is no lower substrate). Note that it is incorrect to interpret this as the drop which occurs when the lower substrate is completely nonwetting and forces a contact angle of π with the lower substrate tangential to the base of the drop. In fact, the insertion of a substrate at the base will alter the configuration of the whole drop.

$D < 0$. In the case where $\alpha > 2/3, D < 0$, inflection occurs, the inclination ϕ passes through a local maximum at $\phi = \pi - \varepsilon\sqrt{-4D}$, and a theoretical new drop can be initiated starting with a neck region opening into a main drop. The positive root of (54) is appropriate before inflection occurs, where ϕ is increasing to $\pi - \varepsilon\sqrt{-4D}$. After inflection, the negative root is the relevant one, and ϕ starts to decrease in value once more.

The scaled Y equation is

$$\frac{d\zeta}{d\Phi} = -\frac{\Phi\xi}{2\xi - \Phi}, \tag{61}$$

with solution

$$\zeta = -\frac{1}{4}\Phi^2 - \frac{1}{4}\Phi\sqrt{(\Phi^2 + 4D)} + D\ln\left(\Phi + \sqrt{(\Phi^2 + 4D)}\right) + c_8 \tag{62}$$

before the point of inflection. After inflection, the solution is

$$\zeta = -\frac{1}{4}\Phi^2 + \frac{1}{4}\Phi\sqrt{(\Phi^2 + 4D)} - D\ln\left(\Phi + \sqrt{(\Phi^2 + 4D)}\right) + \overline{c_8}. \tag{63}$$

As before, it is convenient to rewrite this in the equivalent form as

$$\zeta = -\frac{1}{4}\Phi^2 + \frac{1}{4}\Phi\sqrt{(\Phi^2 + 4D)} + D\ln\left(\Phi - \sqrt{(\Phi^2 + 4D)}\right) + c_8, \tag{64}$$

as continuity at the inflection point now merely requires that the two integration constants be equal (c_8). Matching with the outer solution now gives the following result:

$$c_8 = -\frac{2}{3} - \frac{3}{2}\alpha + 4\alpha \ln 2 - \frac{4}{3}\ln 2 - p_1 + \frac{2}{3}\ln \varepsilon - \alpha \ln \alpha - 3\alpha \ln \varepsilon, \tag{65}$$

where switchback terms have been added as required (see the appendix).

3.6. Lower neck. When inflection occurs ($D < 0$) below the lower layer (Figure 5), the drop now continues via a neck region analogous to that in section 3.1. The relevant scales are

$$X = \varepsilon^3 u, \quad Y = 2\varepsilon + \varepsilon^3 v, \quad P = p/\varepsilon, \quad \phi = O(1). \tag{66}$$

While these are not identical to the scales in section 3.1, we obtain the same leading order balance

$$\frac{du}{d\phi} = -u \cot \phi, \tag{67}$$

$$\frac{dv}{d\phi} = -u, \tag{68}$$

and the corresponding solutions are

$$u = c_9 \csc \phi, \tag{69}$$

$$v = -c_9 \ln \left| \tan \frac{\phi}{2} \right| + c_{10}. \tag{70}$$

Matching with the lower boundary layer solutions now gives

$$c_9 = -D, \quad c_{10} = D \ln \varepsilon + \frac{D}{2} + D \ln |D| + c_8, \tag{71}$$

where c_8 is given by (65), and switchback terms have been added as required (see the appendix).

In Figure 10 we compare the asymptotic solutions for the neck and lower boundary layer with the numerical computations based on (5). Note that the error associated with the shift in the location of the neck is within the error bounds of the asymptotic solutions. Recall that as the equations are coupled, there is naturally an accumulation of error: in particular we recall that $P = p/\varepsilon$ and $p = 2 + \varepsilon^2(-1/3 - 2\alpha)$, so the overall error is $o(\varepsilon)$.

$D > 0$. In the case where $\alpha < 2/3, D > 0$, no inflection occurs, the inclination ϕ increases through π, the drop starts to curl up on itself, and a loop rather than a neck forms [12], [15], [16]. The positive root of (54) is appropriate, while the corresponding Y solution is

$$\zeta = -\frac{1}{4}\Phi^2 - \frac{1}{4}\Phi\sqrt{(\Phi^2 + 4D)} + D \ln \left(\Phi + \sqrt{(\Phi^2 + 4D)}\right) + c_8, \tag{72}$$

where matching shows that c_8 is still given by (65),

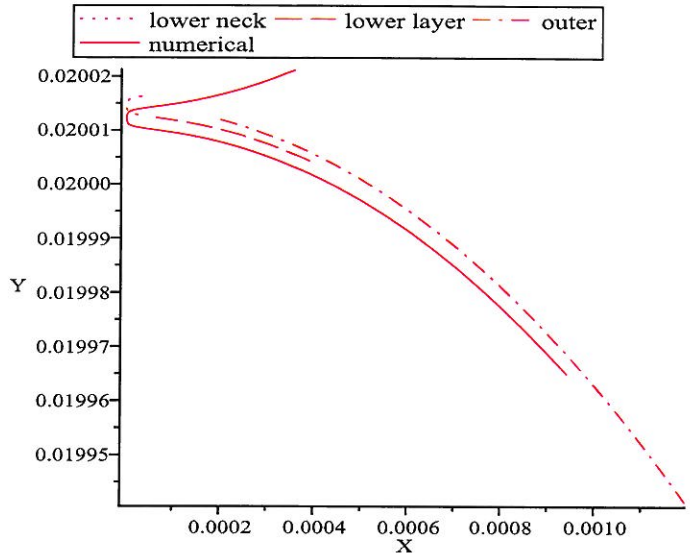

FIG. 10. *Outer, lower boundary layer and lower neck asymptotic solution compared to the numerical solution (solid line) of* (5). $\varepsilon = 0.01, \alpha = 1$.

3.6.1. Lower loop. The boundary layer solutions are valid only near $\phi = \pi$. The initiation of a loop requires the following rescaling:

$$X = \varepsilon^3 u, \quad Y = 2\varepsilon + \varepsilon^3 v, \quad P = p/\varepsilon, \quad \phi = O(1), \tag{73}$$

which leads to the same leading order balances as (67):

$$\frac{du}{d\phi} = -u \cot \phi, \tag{74}$$

$$\frac{dv}{d\phi} = -u, \tag{75}$$

and the corresponding solutions are

$$u = c_{11} \csc \phi, \tag{76}$$

$$v = -c_{11} \ln |\tan \phi/2| + c_{12}. \tag{77}$$

In matching with the lower boundary layer solutions, the dependent variables are linked via

$$\phi = \pi - \varepsilon \Phi, \tag{78}$$

and we note that the matching is for $\Phi < 0, \phi > \pi$. For the X matching we find that we require that

$$\frac{c_{11}\varepsilon^2}{\Phi} = \frac{D\varepsilon^2}{|\Phi|}, \tag{79}$$

and for the Y matching we require

(80)

$$2\varepsilon - \varepsilon^3 (c_{11} \ln 2 - c_{11} \ln |\Phi| - c_{11} \ln \varepsilon - c_{12}) = 2\varepsilon + \varepsilon^3 \left(\frac{D}{2} + c_8 + D \ln 2D - D \ln |\Phi| \right).$$

For $\Phi < 0$ this leads to

$$c_{11} = -D, \quad c_{12} = D \ln \varepsilon + \frac{D}{2} + D \ln |D| + c_8, \tag{81}$$

where c_8 is as defined in (65), and switchback terms have been added (see the appendix).

In Figure 11, we compare the asymptotic loop solutions with numerical computations based on (5).

To complete the solutions section, we give an example in Figures 12, 13, and 14 of how the asymptotic solutions mesh together with X, Y plotted against the parameter ϕ.

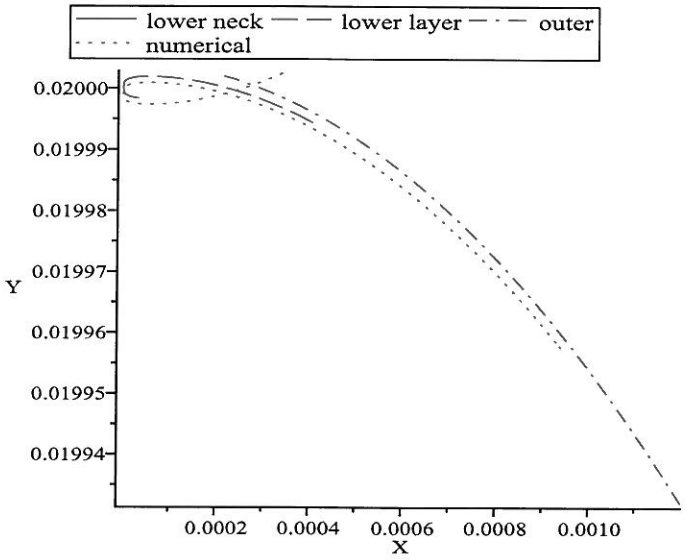

FIG. 11. *Outer, lower boundary layer, and lower neck asymptotic solution compared to the numerical solution (solid line) of* (5). $\varepsilon = 0.01, \alpha = 1/3$.

4. Discussion. Using the method of matched asymptotic expansions, we have obtained asymptotic solutions for the shape of small drops placed on a cone and plate rheometer, sandwiched between the cone and a flat plate (Figure 3). In the physical problem, the influence of the cone and plate enters the problem via a contact angle and, in fact, any axially symmetric object will have a similar effect on the drop shape (the particular details depend on the slope of the object at the point of contact). Changing the angle of the cone and plate rheometer (or changing the slope of an axially symmetric object) will change the effective contact angle but not the overall shape characteristics.

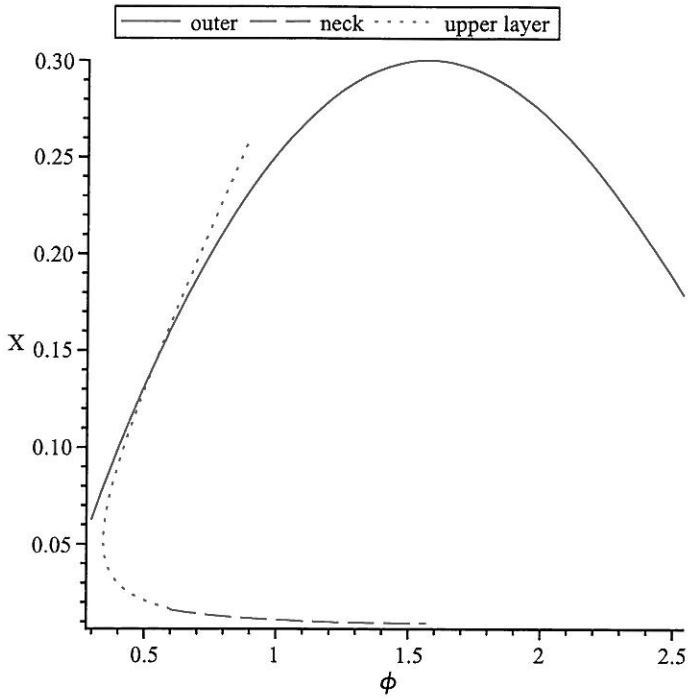

FIG. 12. *Plot of asymptotic X versus ϕ. $\varepsilon = 0.3, \alpha = 1/3$.*

It is interesting to compare the present solutions with previous work. In [12], asymptotic solutions were obtained for a sequence of pendant drops. From a mathematical point of view, the solutions were developed from the base of the drop with initial conditions $X = Y = \phi = 0$. The extra condition at $X(\phi = \pi/2) = \varepsilon$ at the point of maximum bulge was used to fix the unknown pressure P, corresponding to the pressure at the base of the drop. We then *deduced* that the width of the neck at its thinnest point was $2\varepsilon^3/3 + o(\varepsilon^3)$. In the present problem, we started integrating the equations in the neck and, because of the results for the pendant drop, we *assumed* that $X(\phi = \pi/2) = \alpha\varepsilon^3$ was the correct initial condition. However, we tacitly left the $O(1)$ parameter α unspecified with the intention of deducing it from the condition in the main drop that $X(\phi = \pi/2) = \varepsilon$. The solutions indicate that α remains a free parameter at this point, and in fact there is a family of drops, all of which have maximum width $X = \varepsilon$ in the main drop. So unlike the pendant case, fixing the width in the main drop does not fix the minimum width in the neck, and the drop shape is parameterized by two parameters rather than one. Of course, this is an asymptotic theory based on $\varepsilon \to 0$.

It is of immediate interest that the presence of a substrate above (and below) the drop gives rise to qualitatively new drop configurations. The traditional pendant drop is usually assumed to hang from a horizontal ceiling, and this has been shown to give rise to the singular case of the present paper ($\alpha = 2/3$; see [11]). But allowing the drop to be opened out at the top by the cone (Figure 3) apparently gives rise to

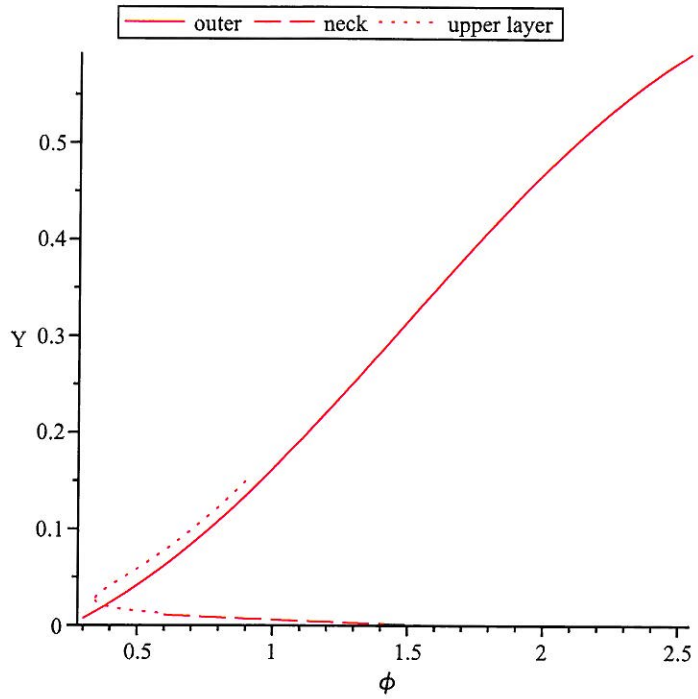

FIG. 13. *Plot of asymptotic* Y *versus* ϕ. $\varepsilon = 0.3, \alpha = 1/3$.

new possible drop shapes.

This may also have repercussions for the stability of liquid bridges (bridges tend to have different stability properties when compared to freely hanging drops, so the presence of substrates at the top and bottom can have profound effects on the profiles). Pendant bridges of two types have been examined in the literature [18], [20]: those with a fixed bottom plate and those for which the lower plate is supported by the liquid. The drops in each case tend to be more stable than the freely hanging case. Chen, Tsampoulos, and Good [2] examine the capillary bridges between parallel and nonparallel plates and show some solutions with multiple bulges. Reports of unstable configurations examined experimentally have been recorded [5] in the limit of slow flow. In capillary problems, unstable solutions can be physically relevant as, for example, what occurs with pinholes in thin films [13]. For any particular film thickness there is an associated pinhole radius: smaller pinholes tend to close over while larger ones tend to open out. Theoretical work on the stability of pendant drops has been carried out in [23] for a certain class of perturbations, though, as pointed out by Finn [4], the procedure used does not correspond to the principle of virtual work . Finn also notes that although multiple drop solutions may be globally unstable, individual portions of the drops can appear as stable configurations which would be physically observed. Further work might use the solutions of this paper as an initial configuration in an initial value problem for the flow in a real cone and plate rheometer.

Note that the approach taken in this paper is a type of semi-inverse formulation in

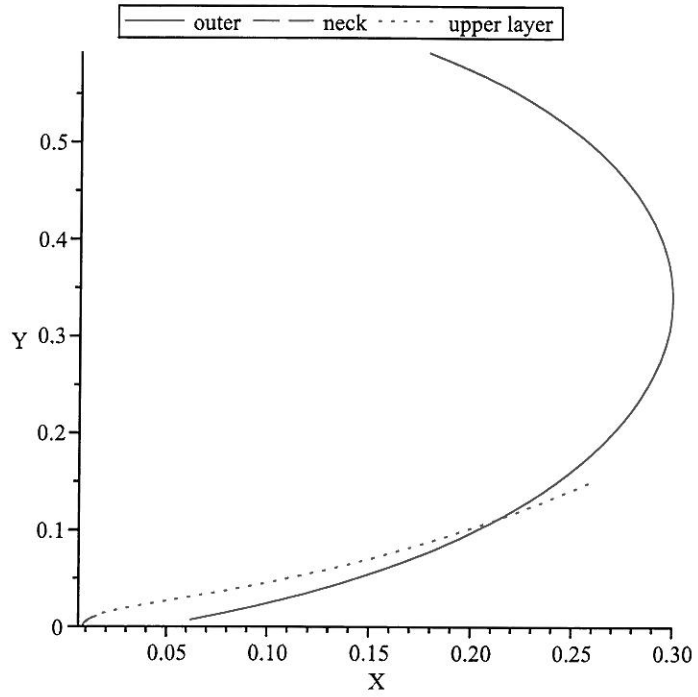

FIG. 14. *X, Y plot corresponding to the parametric plots in Figures* 12 *and* 13. $\varepsilon = 0.3, \alpha = 1/3$.

that it in effect removes the contact angle from the boundary conditions. For example, if we consider Figure 3, then the solutions presented in this paper are started in the neck at the point where the drop becomes vertical. The analysis shows that the width of the neck (and the width of the main drop) are then required to fully determine the solutions. We then develop solutions without any consideration of contact angles; the idea being that we fit in the position of the substrate at the top or bottom by locating it in such a way that the contact angle condition (via the slope of the profile) is satisfied. For example, if the physical situation resembles Figure 3, then the solutions must be continued upward (the neck solutions in section 3.1 are still relevant). One simply allows the inclination ϕ to decrease from $\pi/2$. This allows one to continue the drop profile upward. The caveat is that if the physical situation (i.e., the upper boundary and the contact angle) is such that the slope of the profile approaches the horizontal, the neck solutions will become invalid and another boundary layer must be inserted to continue the solutions. Indeed, if the situation is such that the angle of inclination of the profile at the top is larger than $\pi/2$, the solution above this point should be discarded.

The same idea is illustrated in Figure 4 for the case of a traditional sessile drop. If the actual contact angle at the substrate is $\pi/2$, for example, the theoretical profile is truncated along the dashed line and the solution below this point is discarded. Obviously, by "moving" this horizontal plate up or down, we can create a solution corresponding to a range of contact angles.

The approach in this paper is to compute the drop shapes (approximately) where the contact line positions at the top and bottom of the drop are known. The dimensionless drop volume can then be computed a posteriori, via the elementary computation

$$V^*/L^3 = \pi \int y^2(\phi, \varepsilon) \frac{dx(\phi, \varepsilon)}{d\phi} d\phi,$$

and this allows one, in principle, to compute the drop shape corresponding to a particular volume. A related problem, which we are currently examining, is to compute the shape of an evolving drop as the cone is lowered toward or raised from the plate. In the quasi-static approximation, the solutions of this paper can be used to piece together the changing profile. The associated Stokes' flow problem can certainly be solved numerically, but an analytical approach may also bear fruit. The novel solutions predicted in this paper, in particular the different cases $D = 0, D < 0, D > 0$ of section 3.5, need to be tested experimentally. In fact, this would make a nice microgravity experiment. It is possible that these static solutions are quite difficult to attain in practice. In the spirit of the problem described above, such shapes may be attainable in a careful experimental setting where a cone is lowered toward and raised from the plate of a rheometer. The dynamic processes are hysteretic, and the attainment of any particular configuration may be dependent on such effects and whether contact lines become pinned (or not) on surface impurities [9], [6].

Appendix.

Switchback terms. On examining (23) we find that matching apparently demands that

$$-\alpha\varepsilon^3 (-\ln 2 + \ln \phi) = \varepsilon^3 \left(\frac{\alpha}{2} + c_1 - \alpha \ln 2 - \alpha \ln \phi + \alpha \ln \varepsilon \right). \tag{82}$$

As c_1 is a constant, such a result is impossible because of the extra term proportional to $\varepsilon^3 \ln \varepsilon (\gg \varepsilon^3)$. Such terms are quite common in matched asymptotics [8] and indicate that the form of the series solution for the upper boundary layer solution (23) is not quite correct. In obtaining (23), it was assumed that

$$Y \sim \varepsilon^3 Y_0, \tag{83}$$

but the matching indicates that in fact the series should be of the form

$$Y \sim \varepsilon^3 \ln \varepsilon Y_{\mathrm{SW}} + \varepsilon^3 Y_0. \tag{84}$$

Substituting into the relevant equation (6), it becomes clear that

$$\frac{dY_{\mathrm{SW}}}{d\phi} = 0 \Longrightarrow Y_{\mathrm{SW}} = \text{constant}. \tag{85}$$

From the point of view of matching, this means that we can add any multiple of $\varepsilon^3 \ln \varepsilon$ to solution (23), and we do so in order to satisfy the matching condition. The result is presented in (24) but it should be understood that the extra lower order switchback terms have been obtained independently and then have been absorbed into the "constant" c_1 for convenience of presentation.

REFERENCES

[1] F.V. ATKINSON AND L.A. PELETIER, *Bounds for vertical points of solutions of prescribed mean curvature equations*, Proc. Roy. Soc. Edinburgh Sect. A, 112 (1989), pp. 15–32.

[2] T. CHEN, J.A. TSAMPOULOS, AND R.J. GOOD, *Capillary bridges between parallel and non-parallel surfaces and their stability*, J. Colloid Interface Sci., 151 (1992), pp. 49–69.

[3] P. CONCUS AND R. FINN, *The shape of a pendent liquid drop*, Philos. Trans. Roy. Soc. London Ser. A, 292 (1978), pp. 307–340.

[4] R. FINN, *Equilibrium Capillary Surfaces*, Grundlehren Math. Wiss. 284, Springer-Verlag, New York, 1986.

[5] S. GAUDET AND G.H. MCKINLEY, *Extensional deformation on non-Newtonian liquid bridges*, Comput. Mech., 21 (1998), pp. 461–476.

[6] P.G. DE GENNES, F. BROCHARD-WYART, AND D. QUÉRÉ, *Capillarity and Wetting Phenomena: Drops, Bubbles, Pearls, Waves*, Springer-Verlag, New York, 2004.

[7] S. HARTLAND AND R.W. HARTLEY, *Axisymmetric Fluid Liquid Interfaces*, Elsevier, New York, 1976.

[8] P.A. LAGERSTROM AND R.G. CASTEN, *Basic concepts underlying singular perturbation techniques*, SIAM Rev., 14 (1972), pp. 63–120.

[9] G.D. NADKARNI AND S. GAROFF, *An investigation of microscopic aspects of contact angle hysteresis: Pinning of the contact line on a single defect*, Europhys. Lett., 2 (1992), pp. 523–528.

[10] V.A. NEMCHINSKY, *Size and shape of the liquid droplet at the molten tip of an arc electrode*, J. Phys. D: Appl. Phys., 27 (1994), pp. 1433–1442.

[11] S.B.G. O'BRIEN, *On the shape of small sessile and pendant drops by singular perturbation techniques*, J. Fluid Mech., 233 (1991), pp. 519–539. 26.

[12] S.B.G. O'BRIEN, *Asymptotic solutions for double pendant and extended sessile drops*, Quart. Appl. Math., 52 (1994), pp. 43–48.

[13] S.B.G. O'BRIEN, *Asymptotics of a pinhole*, J. Colloid Interface Sci., 191 (1997), pp. 514–516.

[14] S.B.G. O'BRIEN, *Asymptotics of a series of pendant drops*, SIAM J. Appl. Math., 62 (2002), pp. 1569–1580.

[15] S.B.G. O'BRIEN, *Asymptotics of self intersecting solutions of the pendant drop equations*, ZAMM Z. Angew. Math. Mech., 84 (2004), pp. 158–170.

[16] S.B.G. O'BRIEN, *Further self-intersecting loop solutions of the pendant drop equations*, Proc. Roy. Irish Acad., 106A (2006), pp. 63–84.

[17] S.B.G. O'BRIEN AND B.H.A.A. VAN DEN BRULE, *Shape of a small sessile drop and the determination of contact angle*, J. Roy. Soc.: Faraday Trans., 87 (1991), pp. 1579–1583.

[18] J.F. PADDAY, G. PETRE, C.G. RUSU, J. GAMERO, AND G. WOZNIAK, *The shape stability and breakage of pendant liquid bridges*, J. Fluid Mech., 352 (1997), pp. 177–204.

[19] S.W. RIENSTRA, *The shape of a sessile drop for small and large Bond number*, J. Engrg. Math., 24 (1990), pp. 193–202.

[20] L.A. SLOBOZHANIN AND J.M. PERALES, *Stability of liquid bridges between equal disks in an axial gravity field*, Phys. Fluids A, 5 (1993), pp. 1305–1314.

[21] LORD K. W. THOMSON, *Capillary attraction*, Nature, 34 (1886), pp. 270–272, 290–294, 366–369.

[22] M. VAN DYKE, *Perturbation Methods in Fluid Mechanics*, Appl. Math. Mech. 8, Academic Press, New York, 1964.

[23] H.C. WENTE, *The stability of the axially symmetric pendent drop*, Pacific J. Math., 88 (1980), pp. 421–470.